AN ANALYSIS OF THE ORBITAL EVOLUTION OF LAGEOS FROM SEPTEMBER 1983 TO OCTOBER 1984

A Caporali

Dipartimento di Fisica "G. Galilei"

Università di Padova

F Palutan, A Cenci, M Fermi & R M Montereali

Telespazio S.p.a.- Roma

ABSTRACT

During the MERIT Campaign (September 1983 to October 1984) promoted by the International Astronomical Union and the International Union for Geodesy and Geophysics, the orbit of LAGEOS was covered by an unprecedented network of laser stations. The observations collected and made available through the NASA-Data Information Service and University of Texas form a unique data base for investigations in orbit dynamics and solid earth sciences. This paper concentrates on the dynamics of LAGEOS during the 14 month of the MERIT Campaign. Our goal has been to detect and attempt to interpret unmodeled effects in the evolution of the orbit.

Satellite laser ranging data are sufficiently precise to permit the investigation of signals of decimetric amplitude. The major challenge encountered at this sensitivity is that systematic errors in the orbital parameters, particularly inclination and node, are of the same order of magnitude as, and to some extent correlated with, uncertainties in the Earth Orientation Parameters and the coordinates of the laser tracking stations. Consequently, studies of orbital dynamics become intimately related with research in solid earth physics and geodynamics (distorsion of the tracking network), in geodesy and fundamental astronomy (definition and orientation in space of a conventional terrestrial reference system).

In our approach we have adopted state-of-the-art geopotential, earth and ocean tides and direct three-body perturbations. We have compressed the data into a "normal point" format and have used the NASA-GSFC program GEODYN to compute least squares adjustments to the orbital elements, Earth Orientation Parameters and station coordinates in a two-step approach.

In the first phase we do monthly solutions of the six orbital parameters and of one along-track residual acceleration. The Earth Orientation Parameters are given the values independently provided by the VLBI network IRIS. The station coordinates are left unadjusted at this stage. In this way adjustments of the orbital elements can be estimated in a consistent reference system. The novelty of our approach is that we determine the ability of the adopted force model to predict monthly changes in the orbital parameters. Previous studies on the evolution of LAGEOS orbit have rather concentrated on the comparison of estimated orbital parameters with those predicted by a long term ephemeris. We discuss our results in the context of recent theoretical developments on geophysical causes of perturbation on satellite orbits.

In the second phase of analysis we use GEODYN in the "multi-arc" mode to estimate the Earth Orientation Parameters at five day intervals and station coordinates. The improved values are back-substituted into the normal equations to refine the orbital fits.

This part of the analysis yields estimates at three month intervals of the baselines. We discuss the time series of the european baselines in the context of the ongoing WEGENER-MEDLAS Campaign.

We conclude with an error analysis done with the NASA GSFC program ORAN in order to have an indication of the effect of model biases in the orbit determination.

1. INTRODUCTION

This year LAGEOS has entered its second decade of operation and more than ever it lends itself to studies of precision orbit determination for at least two reasons: first, because the design of the satellite, the choice of the orbit and the work done by several groups during the first decade permit the real trajectory to be reproduced by an analytic curve to high accuracy; second, because in the past years, and particularly in response to the MERIT project (Ref. 27), some 30 stations have contributed to a coverage of the LAGEOS passes sufficiently dense and of high quality to support precision studies of the orbit. And, in this respect, the contribution of the European stations has been determinant in filling many gaps in the data set.

Since its launch, in May 1976, LAGEOS and its orbit have drawn the attention of several research groups. Smith and Dunn (Ref.21) analyzed 32 month of data since launch. For each 30-day arc they evaluated the Keplerian elements of the satellite at the first point of maximum latitude and compared them with those derived from one 32 month reference orbit. In this way they were able to identify systematic trends in the unmodeled changes of the major semi axis, both secular and periodic, and unmodeled periodic changes in the eccentricity and inclination. The explanation of periodic changes in

Proceedings of the Second International Symposium on Spacecraft Flight Dynamics, Darmstadt, FR Germany, 20–23 October 1986 (ESA SP-255, Dec. 1986)

the major semi-axis with amplitude within 10 cm. has been attempted by means of a model for the Earth specular and diffuse albedo with hemispherical asymmetry (Ref. 2) or atmospheric drag (Ref. 18), or thermal anisotropic emission (Ref. 3). Charge drag can produce both secular and periodic perturbations on the major semi-axis (Ref.1). The development of a deterministic model suffers from uncertainties in the charging mechanism and in the plasmasphere environmemt but there seems to be a precise correlation between LAGEOS residual acceleration along track and the orientation of the orbital plane relative to the sun. Smith and coll. (Ref. 22) reanalyzed the LAGEOS orbital evolution from May 1976 to end of 1982. They in particular showed that the spectrum of the time series of successive estimates of a residual along track acceleration has remarkable similarities with the spectrum of the solar tidal periodicities of the orbit. By appropriate model of the major tidal perturbations, they also showed that systematic variations of the node relative to a reference orbit integrated for the 6.5 years were confined to within ±50 milliarcsec, after removal of a secular trend probably caused by uncertainties in the even zonal harmonics.
Evidence of the effect of post-glacial rebound on the second zonal harmonic (Ref. 25) was also visible as a curvature of the node residuals.
Schutz and coll.(Ref. 19) have pointed out the importance of defining an appropriate coordinate system as basic prerequisite for the description of the motion of any dynamical system. They have produced time series of the Earth Orientation Parameters at three day intervals which agree with analogous dual baseline VLBI estimates to within the estimated accuracy (2 marcsec for x, y; 0.2 millisec for UT1) of the measurements (1 marcsec = 10^{-3} arsec).In this report we concentrate on a relatively short time span: 15 month, from September 1983 to November 1984. However the data distribution in this period is dense, uniform and of high quality. In Section 2 we review a number of perturbations acting on the satellite orbit. In Section 3 we define our models for the reference systems and the spacecraft dynamics, and present the method of analysis . Section 4 contains the results: we discuss the accuracy of our model in terms of discontinuities of the contiguous monthly orbital arcs in which we have divided the 15 month of data. The dependence of the orbital discontinuities on the model adopted in the data analysis is investigated by means of an error analysis done with the ORAN program. An improved solution for the Earth Rotation Parameters is presented and compared with an independent VLBI solution and other Satellite Laser Ranging solutions. We finally present a time series of european baselines relevant to the WEGENER MEDLAS Campaign and discuss their repeatibility.

2. GRAVITATIONAL PERTURBATIONS ON LAGEOS ORBIT

2.1 Perturbations due to the earth field

To analyze the spectral structure of the gravitational perturbations on LAGEOS we introduce the complex perturbing potential (cf. e.g. Ref. 9) of the earth:

$$U = \sum_{l=2}^{\infty} \sum_{m=0}^{l} U_{lm} \qquad (1)$$

where

$$U_{lm} = \sum_{p=0}^{l} \sum_{q=-\infty}^{\infty} U_{lmpq} \qquad (2)$$

and

$$U_{lmpq} = \frac{Gm}{a}\left(\frac{a_e}{a}\right)^l F_{lmp}(I)\, G_{lpq}(e)\, C_{lm} \exp i\{\gamma_{lmpq} - [l-(-1)^{l-m}]\pi/4\} \qquad (3)$$

We define:
Gm as the earth gravitational mass times the gravitational constant G,
a_e the earth radius,
a,I,e the major semi-axis, inclination and eccentricity of LAGEOS
C_{lm} the normalized complex Stokes coefficents.
The center of mass of the earth is the origin of the reference system, so that $C_{10}=0$.
The phase of the perturbation is

$$\gamma_{lmpq} = (l-2p)\omega + (l-2p+q)M + m(\Omega - \vartheta) \qquad (4)$$

where ω, M, Ω and ϑ are respectively the longitude of perigee, the mean anomaly, the right ascension of the ascending node and the sidereal time. F_{lmp} are trigonometric polynomials in the inclination and G_{lpq} are polynomials in eccentricity (Ref. 9). Those entering the perturbation with l=2 are :

$$F_{221}(I) = \frac{3}{2}\sin^2 I$$
$$F_{211}(I) = -\frac{3}{4}\sin 2I$$
$$F_{201}(I) = \frac{3}{4}\sin^2 I - \frac{1}{2}$$
$$G_{210}(e) = (1-e^2)^{-3/2} \qquad (5)$$

The equations for the perturbations of the orbital elements are

$$\frac{da}{dt} = \frac{2}{na}\frac{\partial[Re(U)]}{\partial M}$$

$$\frac{de}{dt} = \frac{(1-e^2)^{1/2}}{na^2 e}\left\{(1-e^2)^{1/2}\frac{\partial[Re(U)]}{\partial M} - \frac{\partial[Re(U)]}{\partial \omega}\right\}$$

$$\frac{dI}{dt} = [na^2(1-e^2)^{1/2}\sin I]^{-1}\left\{\cos I\,\frac{\partial[Re(U)]}{\partial \omega} - \frac{\partial[Re(U)]}{\partial \Omega}\right\}$$

$$\frac{d\Omega}{dt} = [na^2(1-e^2)^{1/2}\sin I]^{-1}\frac{\partial[Re(U)]}{\partial I}$$

$$\frac{d\omega}{dt} = [na^2(1-e^2)^{1/2}]^{-1}\cot I\frac{\partial[Re(U)]}{\partial I} - \frac{(1-e^2)^{1/2}}{na^2 e}\frac{\partial[Re(U)]}{\partial e}$$

$$\frac{dM}{dt} = n - \frac{(1-e^2)^{1/2}}{na^2 e}\frac{\partial[Re(U)]}{\partial e} - \frac{2}{na}\frac{\partial[Re(U)]}{\partial a} \qquad (6)$$

where Re(U)denotes the real part of U and $n = \sqrt{Gm/a^3}$ is the Keplerian angular velocity of the satellite. By inserting the earth perturbing potential into the Lagrange equations one verifies that long periodic (>2π/n) gravitational perturbations exist for all elements, except for the major semi-axis a, where the period is $2\pi/(1-2p+q)n$. In particular long periodic perturbations start from degree l=2 for the mean anomaly M, the longitude of node Ω and the perigee ω and (with m=0) inclination I; and from degree l=3 for the eccentricity e, due

to the property of the G polynomials that $G_{20-2} = G_{222} = 0$.
So, for instance, at l=2 there exist diurnal (m=1) and semidiurnal (m=2) perturbations in inclination

$$\dot{I}_{2m1O} = -\, m\, n\left(\frac{a_e}{a}\right)^2 \frac{F_{2m1}\,(I)}{(1-e^2)^2 \sin I} \quad \mathrm{Re}(C_{2m}$$

$$\exp i\{m(\Omega-\vartheta)-[1-(-1)^{2-m}]\pi/4\}) \qquad (7)$$

As to the node, for m=0 it exhibits the known secular drift due to the zonal C_{20} with diurnal (m=1) and semidiurnal (m=2) periodic perturbations superimposed

$$\dot{\Omega}_{2m1O} = -\, n\left(\frac{a_e}{a}\right)^2 \frac{\partial F_{2m1}/\partial I}{(1-e^2)^2 \sin I} \quad \mathrm{Re}(C_{2m} \exp i\{m(\Omega-\vartheta)$$

$$-\,[1-(-1)^{2-m}]\pi/4\}) \qquad (8)$$

Long periodic perturbations (that is with period $2\pi/(1-2p)\dot{\omega}$) exist for zonal harmonics (m=0) with l>3. The small factor $(a_e/a)^l$ in the amplitude is partly compensated by the division by $(1-2p)\dot{\omega}$, instead of $m\dot{\vartheta}$. The perturbations associated to even zonal harmonics tend to have larger amplitudes than for odd zonals, due to the property that $G_{lpq} \sim (\text{eccentricity})^{|q|}$.
As to the non zonal harmonics (m>0) resonance occurs when

$$l-2p+q>0$$
$$(1-2p+q)(\dot{\omega}+\dot{M}) + (\dot{\Omega}-\dot{\vartheta}) \sim 0 \qquad (9)$$

LAGEOS makes approximately 6.4 revolutions per day, so that it is in shallow resonance with harmonics of order m=6, and, to a lesser extent, m=5 and 7. For nearly circular orbits the resonant, short periodic perturbations and the m-daily perturbations have a dominant frequency $(1-2p+q)(\dot{\omega}+\dot{M}) + m(\dot{\Omega}-\dot{\vartheta})$ and $q\dot{\omega}$ as slow modulating frequency (Ref. 11).

2.2 Perturbations due to the field of the sun and the moon and to the tides

In the coupling of the earth potential with the potential of the sun or the moon the dependence of the resulting potential on sidereal time can cancel. Long period perturbations result from the combination of the proper frequency of the satellite's node motion (1049 days for LAGEOS) and the proper frequencies of the orbital motion of the sun and moon. The appropriate coordinates are ecliptical and the resulting perturbing potential can be represented in this frame (Ref. 8). The period of the long periodic perturbations on LAGEOS can be computed using the formula

$$T(\text{days}) = 1/\left[\frac{m}{1049} + \frac{-m+n_2-5}{27.2} - \frac{n_3-5}{365} - \frac{n_4-5}{3232}\right.$$

$$\left. - \frac{n_5-5}{6805}\right] \qquad (10)$$

where $n_1 = m$, n_2, n_3, n_4 and n_5 are the Doodson numbers (n_6 may be neglected as the motion of perihelion involves far too long time scales).
Table 2.1 summarizes the longest period perturbations on LAGEOS orbit. Following Ref. 9 we have introduced the amplitude of each tidal constituent

$$A = \frac{Gm'}{a'}\left(\frac{a_e}{a'}\right)^l (2-\delta_{om})\,\frac{(l-m)!}{(l+m)!}\,F_{lmp}\,(I')\,G_{lpq}\,(e') \qquad (11)$$

in terms of the ecliptic elements a', I', e' of the perturbing body. Besides the direct effect on the orbit of the satellite, the sun and the moon have an indirect effect, consisting of tidal perturbations of the solid earth and of the oceans.
Assuming that at the earth surface the earth potential responds linearly to the tidal perturbation, the perturbed part of the potential can be written as (Ref. 9):

$$\Delta U_{lm} = k_l\left(\frac{a_e}{r}\right)^{2l+1}\frac{Gm'}{r'}\left(\frac{r}{r'}\right)^l (2-\delta_{om})\,\frac{(l-m)!}{(l+m)!}$$

$$.P_{lm}(\sin\varphi')\, e^{-im\lambda'}$$

$$.P_{lm}(\sin\varphi)\, e^{im\lambda} \qquad (12)$$

where r, φ, λ and r', φ', λ' are geocentric spherical equatorial coordinates of the satellite and, respectively, the perturbing body; k_l is the Love number of degree l.
The corresponding perturbation of the earth potential can be described as a perturbation in the normalized Stokes parameters C_{lm}.
Defining

$$\Delta C_{lm} = N_{lm}^{-1}\,\mu\left(\frac{a_e}{r}\right)^{l+1} k_l\left(\frac{r}{r'}\right)^l \cdot (2-\delta_{om}) \cdot$$

$$\frac{(l-m)!}{(l+m)!}\,P_{lm}(\sin\varphi')\, e^{-im\lambda'} \qquad (13)$$

$$N_{lm} = \frac{(l-m)!\,(2l+1)(2-\delta_{om})}{(l+m)!} \qquad (14)$$

$\mu = m'/m$ mass ratio

the tidally distorted gravitational potential can be written in geocentric equatorial spherical coordinates:

$$U_{lm} + \Delta U_{lm} = \frac{Gm}{r}\left(\frac{a_e}{r}\right)^l \left(C_{lm} + \sum_{\bullet,D} \Delta C_{lm}\right)$$

$$. e^{im\lambda} P_{lm}(\sin\varphi) \qquad (15)$$

The periods of the tidal perturbations on the orbit are the same as the corresponding direct lunisolar perturbations.
The numerical value of the amplitude and phase of ΔC_{lm} depends on solid earth and ocean models. According to the standards recommended for the MERIT project, the solid earth contribution to ΔC_{lm} is computed on the basis of the Wahr model (Ref. 26). The Love number k_2 becomes a function of the tidal constituent. Similarly for the ocean tides the periodic variations of the Stokes coefficents C_{lm} have been computed for a number of tidal constituents on the basis of the Schwiderski model (Ref. 20).
The amplitudes of the perturbations of the orbital elements are computed using the Lagrange equations. For l=2 and q=0, the part of the perturbation on the orbit time scale is removed when p=1 and there are no long periodic perturbations on the eccentricity, as the disturbing potential becomes independent of ω and M. Therefore we consider perturbations in inclination and node (tab.2.2). They are summarized in Table 2.3.
The contributions to I and Ω from the solid earth tides are computed using a frequency independent k_2=0.29 with frequency dependent corrections δk from Wahr model and amplitudes of the tidal potential from the Cartwright and Tayler and Cartwright and Edden expansion of the tide generating

(as quoted in Ref. 12).
As discussed by Cazenave and coll. (Ref. 6) and Goad (Ref. 8), the periodic perturbations in inclination produce an indirect periodic effect in the J_2-induced node precession

$$\dot{\Omega}_{J2} = \frac{3n\ C_{20}}{2(1 - e^2)^2}\left(\frac{a_e}{a}\right)^2 \cos I\ (t) \qquad (16)$$

with

$$I(t) = I_0 + \Sigma_s\ \ I_s\ \cos(\omega_s\ t + \varphi_s) \qquad (17)$$

s labels the spectral terms in tab. 2.1, ω_s and φ_s are the corresponding frequency and phase and I_0 is the nominal inclination at t=0. This indirect effect has not been considered in the compilation of tab. 2.3.

3. MODEL AND THE METHOD OF ANALYSIS

The data analysis is done with the NASA-GSFC program GEODYN (Ref. 15). GEODYN can work as an orbit estimator, in the sense that it adjusts -in the weighted least squares sense- orbital parameters (6-dimensional state vectors and residual accelerations) of different arcs keeping common parameters (geopotential, station coordinates, Earth Orientation Parameters, tidal coefficents....) fixed at nominal values. GEODYN can also work in multiarc mode: the weighted least squares estimates of the orbital parameters for all arcs are back substituted into the normal equations to produce a unique estimate of a common set of parameters.
In our analysis we have combined GEODYN with the tidal model recommended for the MERIT Campaign (Wahr's solid earth tides: O_1, P_1, Res_2, K_1, Res_1, ψ_1, M_2, S_2, K_2; Schwiderski's ocean tides of even and odd orders up to degree 6: P_1, K_1, O_1, N_2, M_2, S_2, K_2; S_2 ocean tide coefficents of degree and order 2 corrected for atmospheric tide with appropriate sign).The gravity field PGS 1680 (Ref. 11), rather than MERIT's GEM-L2 (Ref. 10) was adopted, in order to have a field which both has $(C,S)_{21}$ set to the MERIT recommended values and is tailored on LAGEOS. Although we have focused on one particular field, we think that other fields, in particular GRIM3 L1 (Ref. 16) should be considered in future analyses. The Earth Orientation Parameters have been given as initial values those independently provided by the VLBI network IRIS (Series 85 Oct. 26 on IRIS Bulletin n.21 of November, 1985). An updated set of coordinates has been used for the tracking stations (M. Torrence, private communication). Table 3.1 summarizes the adopted model.
The data have been divided into arcs of 30 days. In the first part of the analysis, seven parameters (6-dimensional state vector and one residual acceleration along track) are adjusted keeping the common parameters fixed at their nominal values. The orbital parameters are estimated at the beginning of each arc, and then propagated 30 days forward, in order to compare them with those estimated in the following arc.
In the second phase of analysis the tracking network (Matera latitude and longitude and GORF latitude fixed) and the Earth Orientation Parameters are adjusted simultaneously with the three sets, each of seven orbital parameters, of three contiguous arcs. In order to avoid correlated estimates of node and A1-UT1, we have tested the option of keeping A1-UT1 fixed at the VLBI value when the orbit is adjusted, leaving it otherwise freely adjustable at 5 day intervals.

4. RESULTS

4.1 Orbital analysis from a nominal terrestrial system

The first part of this section summarizes our results on the ability of the adopted model to predict changes of the four orbital parameters a, e, I, Ω. These are more practical parameters to investigate, since the mean anomaly absorbs a variety of random and systematic effects along track and, for a nearly circular orbit, the longitude of perigee is poorly determined. To quantitatively estimate how smoothly consecutive arcs match each other we compute the part of each orbital parameter left unaccounted after 30 days of propagation. Changes in major semi-axis (fig. 4.1) are clearly systematic but confined within +/-5 mm. This indicates that our model for the evolution of the major semi-axis is accurate, in the sense of repeatibility, to 4 parts in 10^{10}, after removal of the empirical along track term. Similarly, the accuracy of the eccentricity (fig. 4.2) is 5 parts in 10^8. There is a negative bias and a negative autocorrelation on the first five arcs. This feature is however not maintained in the rest of the plot, which appears random.
In the inclination residuals (fig. 4.3) there is a clear trend for which long periodic tidal perturbations are the most likely sources. Only an analysis over a data span of several years can indicate which tidal species is responsible for the trend. The small oscillation superimposed cannot yet be characterized quantitatively. Power spectra of these inclination residuals and of their subsets, after removal of a best fitting straight line, seem to indicate that the power is concentrated in the long period region (> 150 days). If this is real, then table 2.1 shows that the T_2 tide and a couple of small terms in the P_1 group (R_2 and Φ_1) could be likely candidates to account, at least in part, for the residual oscillation. The 280 days oscillation found in a previous investigation (Ref. 4) has disappeared. This suggests that the (2,2) coefficient of the S_2 ocean tide should indeed be corrected for the atmospheric tide, with the appropriate sign.
When the dominant linear trend in fig. 4.3 is removed, the accuracy of the model of inclination is better than 2 parts in 10^8.
The node residuals (fig. 4.4) are confined within +/-7 marcsec about a positive mean of 20 marcsec. The first three points are linearly autocorrelated. The remaining eleven still maintain some structure. Because our method of analysis uses changes of the orbital elements, a constant mean value indicates the presence of a linear drift of the "true" node relatively to that predicted by our model. This means that our model "falls short" of about 20 marcsec in rotating the node during a 30 day period.
Using the NASA GSFC program ORAN we verified that the uncertainties estimated for the zonals (m=0) of GEM-L2 can produce effects at the centimeter level in all the orbital parameters, not just the node. Similarly, the estimated uncertainties of the tesserals (l>1, m>0), in particular the nearly resonant C(7,7) term, can change the semi major axis by several cm.. Using ORAN we also investigated the effect on the orbit determination of biases in the coordinates of the stations forming our tracking network. We found that biases equal to one formal standard error estimated by GEODYN can produce changes in the orbital parameters relative to those which would be obtained with no bias. For example,

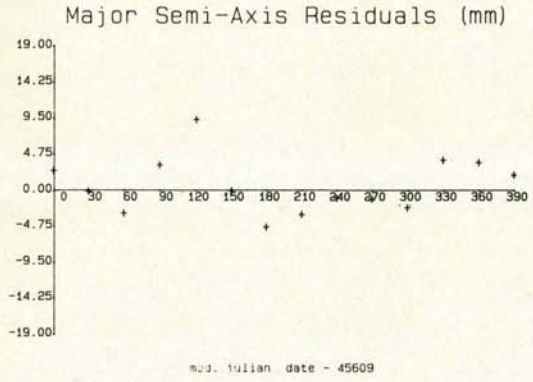

Figure 4.1: unmodelled changes of the major semi-axis relative to predictions, after subtraction of the effect of an empirical along track acceleration constant during the 30-day arcs .

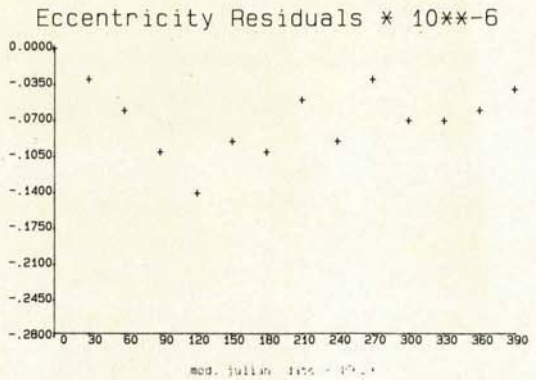

Figure 4.2: unmodelled changes in orbital eccentricity relative to predictions.

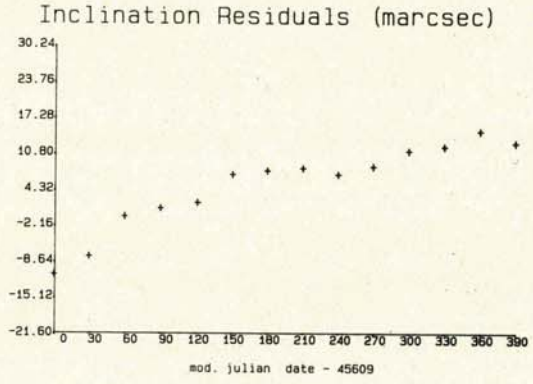

Figure 4.3: unmodelled changes of the inclination relative to predictions. The secular term is probably a portion of a long periodic effect of a tidal perturbation. A perturbation with shorter period is also visible.

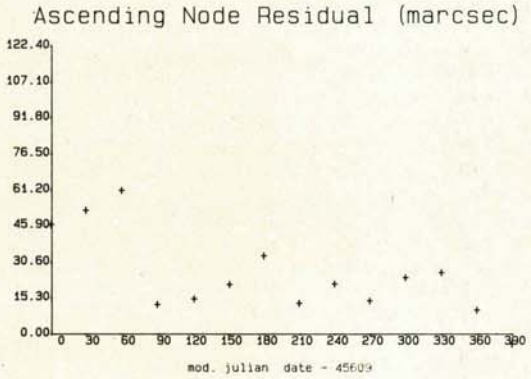

Figure 4.4: unmodelled changes in the right ascension of the ascending node.

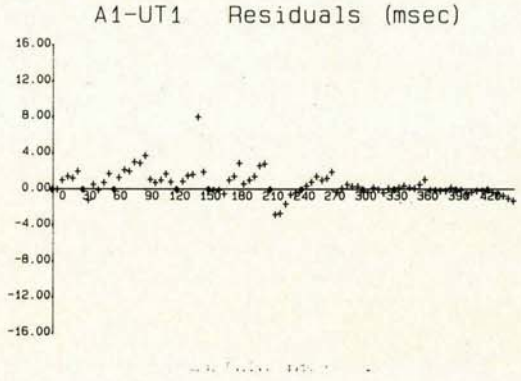

Figure 4.5: differences between our estimates and VLBI(NGS) estimates of AI-UTI. Circled points indicate that our solution was constrained to the VLBI value. Single baseline VLBI observations have been predominant during the first three months of the MERIT campaign.

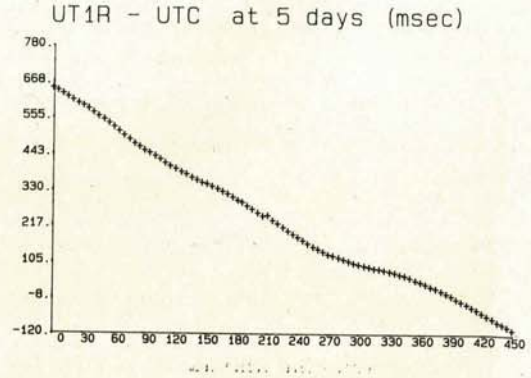

Figure 4.6: difference between UTI and UTC, after subtraction of the effect of 41 short periodic tidal terms.

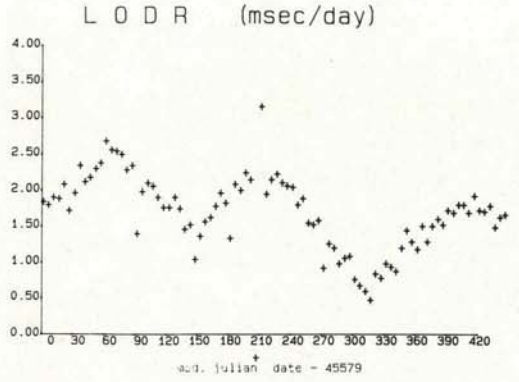

Figure 4.7: excess length of day as computed by numerical differentiation of UTIR-UTC.

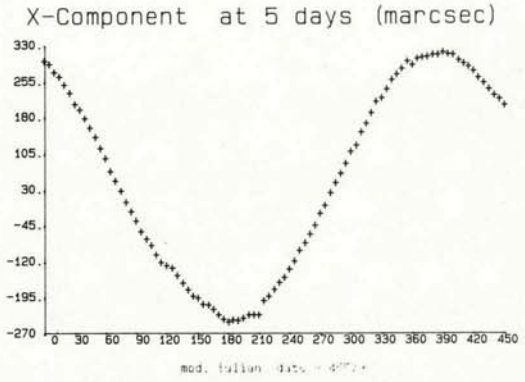

Figure 4.8: estimates of the x component of the instantaneous rotation axis.

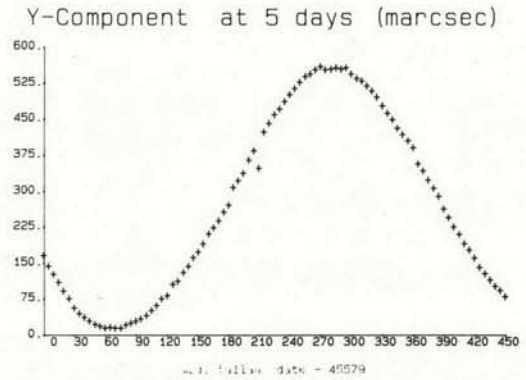

Figure 4.9: estimates of the y component of the instantaneous rotation axis.

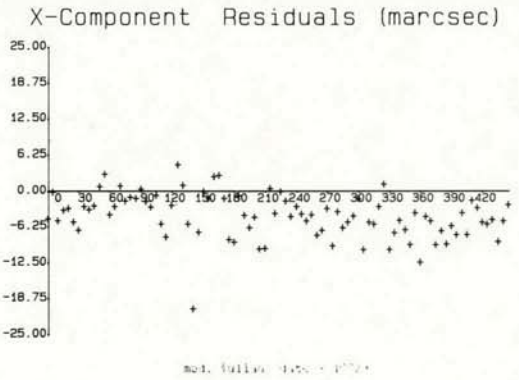

Figure 4.10: difference between our estimates and VLBI(NGS) estimates of the x component of the polar motion. VLBI values are constrained to University of Texas LAGEOS values for single baseline observations.

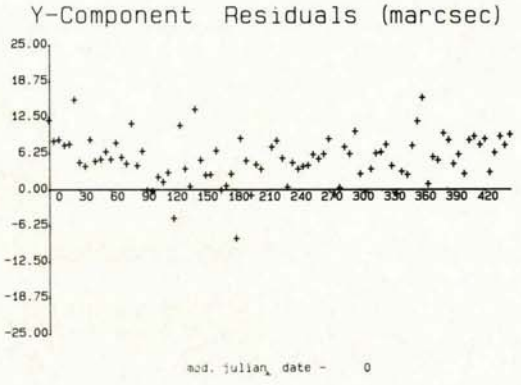

Figure 4.11: difference between our estimates and VLBI(NGS) estimates of the y component of polar motion. See fig. 4.10.

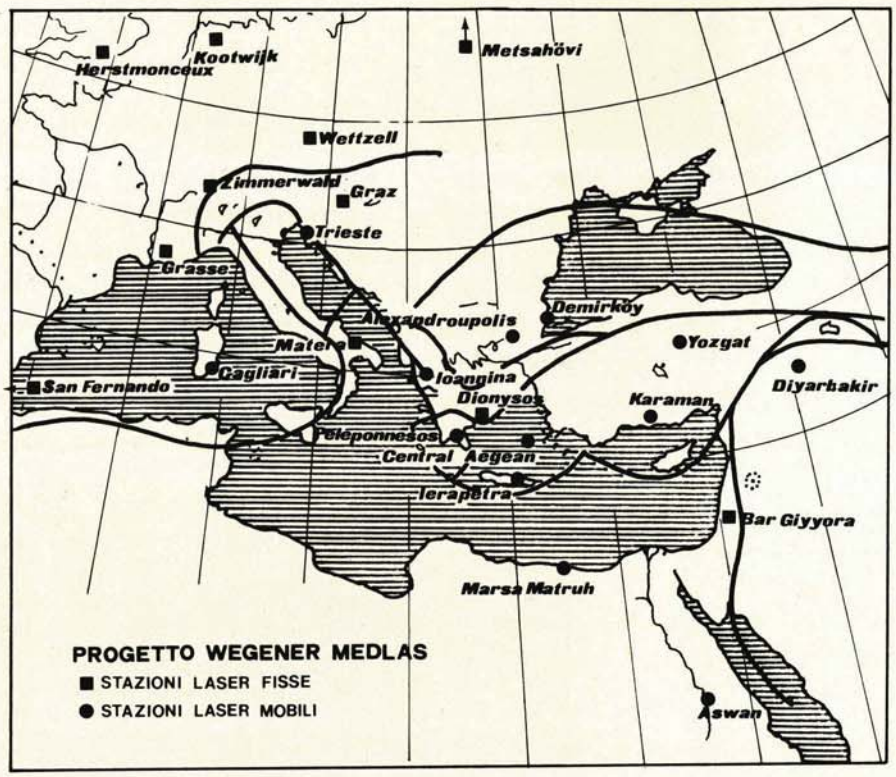

Figure 4.I2: network of fixed and mobile laser systems for the WEGENER - MEDLAS project.

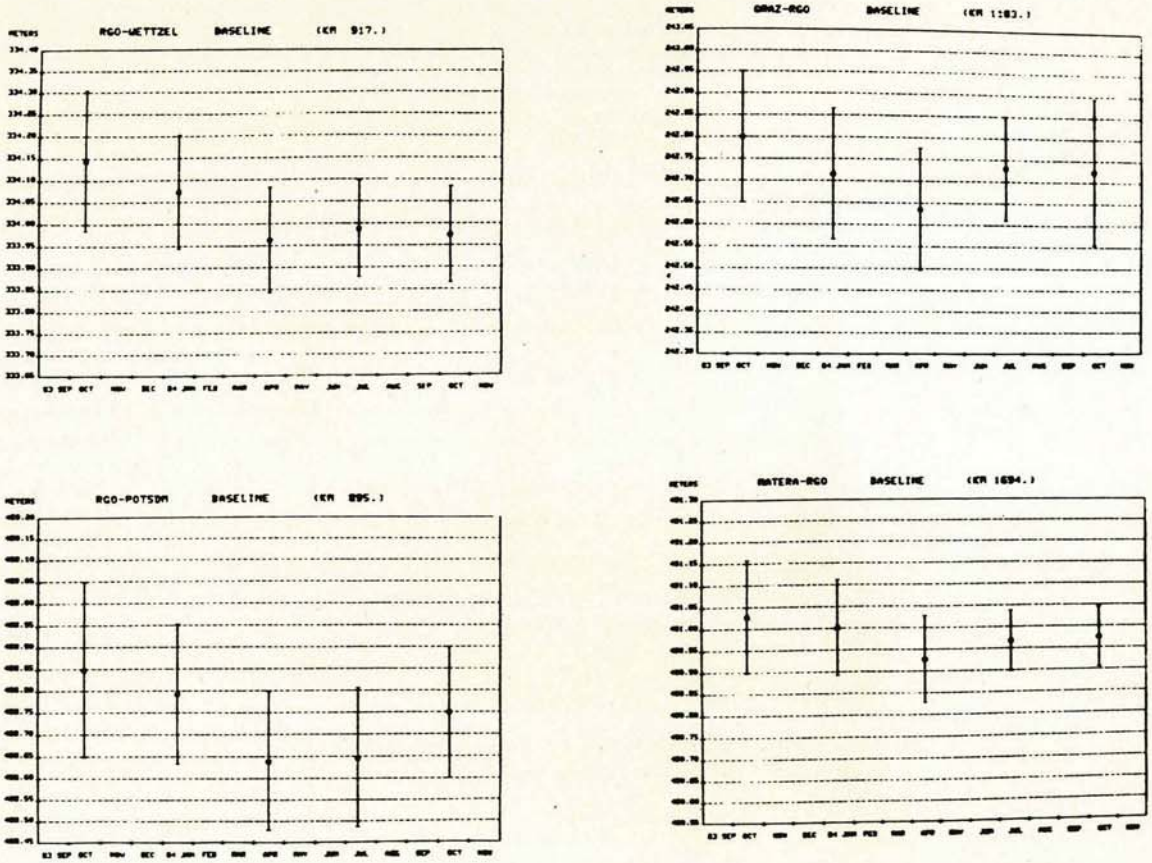

Figure 4.I3: four correlated time series of baselines to Royal Greenwich Observatory

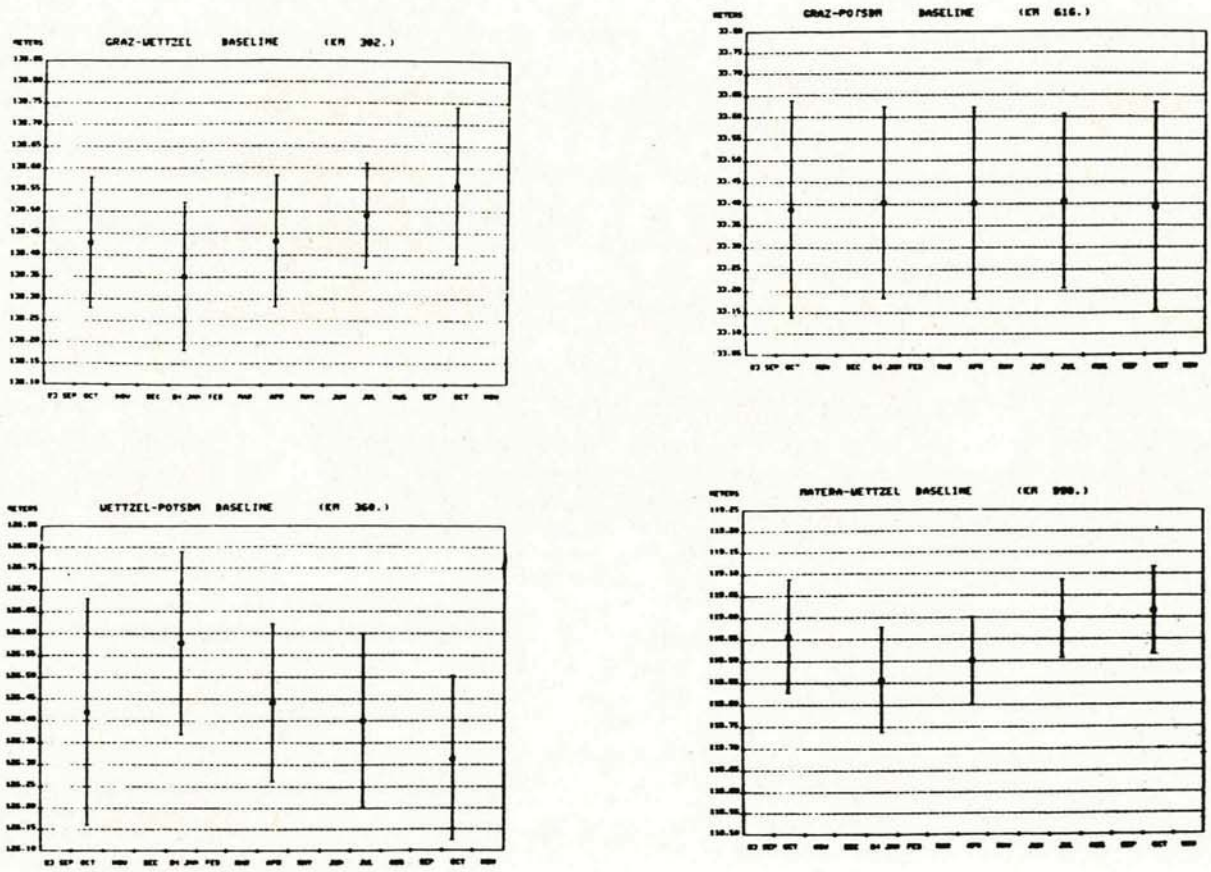

Figure 4.I4: three correlated time serie of baselines to Wettzell and the Graz-Potsdam baseline

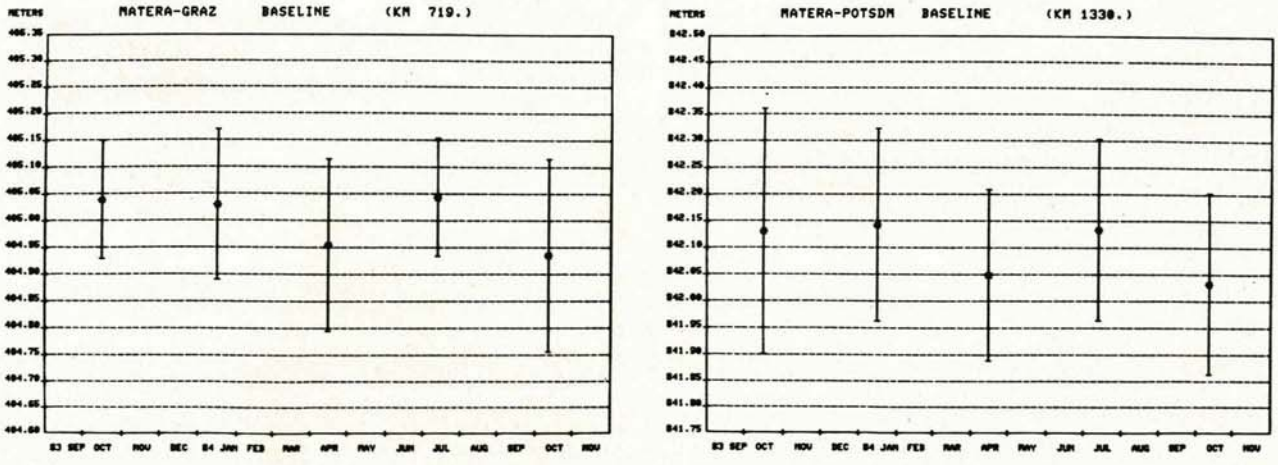

Figure 4.I5: two correlated time series of baselines to Matera with strong north-south component.

we verified that the y coordinate of station 7121 (Huahine) or the x coordinate of station 7122 (Mazatlan) may influence the major semi axis at the mm. level and the eccentricity at 0.07 ppm. The same analysis indicates that biases in the coordinates of the other stations only influence the node and inclination at the marcsec. level.

4.2 Results of the adjustment of the terrestrial system

In the second phase of analysis,the coordinates of the tracking network and the Earth Orientation Parameters have been adjusted simultaneously with the seven orbital parameters The Earth Orientation Parameters are adjusted at 5 day interval centered at the epochs of the BIH Circular D values. In some cases Al-UT1 has been constrained to the VLBI (NGS) value when the orbit is estimated; otherwise it has been left freely adjustable. As fig. 4.5 indicates, the dispersion of our estimates relative to the VLBI estimates is largely independent of this constraint. In the first nine arcs, up to day 270, our estimates are systematically drifting relative to the VLBI estimates. The remaining six arcs give estimates in much closer agreement. Fig. 4.6 represents our estimates for Al-UT1 after removal of Al-UTC, as given by the U.S. Naval Observatory (22.0343817 sec. throughout the MERIT Campaign) and of the effect UT1-UT1R of 41 tidal effects of periods between 5.64 days and 34.85 days (Ref. 24). In fig. 4.7 we have plotted 5-day averages of the excess length of day, computed from the expression (Ref. 17)

$$LODR(t_{i+1}-2.5)= -[(UT1R - UTC)_{t_{i+1}}-(UT1R-UTC)_{t_i}]/5 \qquad (18)$$

The path of the x, y coordinates of the pole is shown in fig. 4.8 and 4.9. Occasional discontinuities at three months intervals are visible, as a consequence of the adjustment of the station coordinates. Figg. 4.10 and 4.11 show the residuals relative to the VLBI(NGS) solution and indicate the existence of a small offset in both coordinates. The relevant statistics are reported in table 4.1 which also contains the statistics of other solutions, as computed in Ref. 23. Last entry (UPTPZ69) is from Ref. 4. Table 4.1 indicates that the offset of our solution relative to VLBI, though non negligible, is smaller than in other solutions. This, in part, is due to the adoption of the MERIT recommended values for $(C,S)_{21}$, but also to the improved tidal model which, as discussed in Sect. 2.1, defines the periodic variations of these coefficients. Another source of discrepancy can be the nominal value chosen for the three station coordinates we held fixed.
A better agreement among the solutions can probably be achieved but may require a frequency resolutionn higher than 5 days, as the rms's are likely to be due to high frequency systematic terms, besides random noise (Ref. 5).
In addition to mean differences between solutions, we have compared estimates of the amplitudes and phases of the annual and Chandler terms. This was done by fitting our time series for x_p, y_p to the curve

$$f(t) = a + c_1 \cos\frac{2\pi}{365.24}t + s_1 \sin\frac{2\pi}{365.24}t + c_2 \cos\frac{2\pi}{432.0}t + s_2 \sin\frac{2\pi}{432.0}t \qquad (19)$$

with t in days since Sept. 2, 1983, 0^h UTC. Our results are summarized in table 4.2. The NGS solution was our "a priori". It covers the same time span (83.09.02- 84.10.31) as our solution and the relevant numbers have been computed by us. The remaining numbers quoted in tab. 4.2 are from Ref.17. The agreement between the solutions obtained with VLBI and SLR techniques is remarkable. Figure 4.12 qualitatively describes the network of satellite laser stations for the WEGENER MEDLAS Campaign. Our data set is obviously too short for looking at changes in the baselines significant from the point of view of crustal deformation. . At this stage we can only investigate the repeatibility of consecutive estimates. For instance, the correlations existing between estimates of baselines joining RGO to Graz, Wettzell, Matera and Potsdam (fig. 4.13) indicate that changes in the coordinates of RGO map very clearly into these baselines . A different type of correlation exists for the baselines joining Wettzell to Matera, Graz and Potsdam, while Graz-Potsdam shows an impressive repeatibility (fig. 4.14). Finally it is remarkable the similarity between the Matera-Graz and the Matera-Potsdam estimates. Because Matera is held fixed and Graz is at an intermediate position relative to Matera and Potsdam, the correlation between two baselines to Matera is perfectly consistent with the repeatibility of the Graz Potsdam baseline: .

5. CONCLUSIONS

The data span selected for this work limits the period of visible unmodeled perturbations from 60 days (Nyquist period) to 420 days. As primary result of this research we estimate that the model we have adopted, based on MERIT standards, has a repeatibility ranging from 4 parts in 10^{10} for the major semiaxis to 2 parts in 10^7 for the node. The residuals have random and systematic character. The frequencies of the systematic component is at least in part in the range of sensitivity of this analysis. The amplitudes cannot yet be estimated reliably. Uncertainties in the tide model cause the inclination and node to contain larger systematics than the major semi axis and eccentricity.
The definition and orientation of the terrestrial system can also affect the determination of the orbital elements. Because the time series of polar motion generated in this work agrees with that independently derived by VLBI to within 5 milliarcsec r.m.s., only the earth rotation rate contributes to systematics in the orbital parameters, especially the high frequency part of the node residuals. The low frequency part is instead dominated by uncertainties in the zonal harmonics.
We find an excellent agreement in both amplitude and phase with the annual and Chandler constituents of polar motion independently derived by other groups.
Consecutive estimates of european baselines have an average repeatibility of 15 cm.. The network is very sensitive and correlations of baseline changes can permit to identify which station is moving relative to others.
This body of results confirms the great potential of satellite laser ranging for work in high accuracy orbit determination and for geophysical studies of the sources of perturbations in satellite orbits.

Acknowledgment: This research is supported by Piano Spaziale Nazionale - Consiglio Nazionale delle Ricerche.

TABLE 2.1 Tidal species and period of their perturbations on LAGEOS (Ref. 13)

Doodson Number	*Symbol*	*Period (days) of orbital perturbation*	*Amplitude A of the tide on Earth ($10^3 m^2/s^2$)*	*Note*
165 565	Res_1	1240		
165 555	K_1	1049	6.356L 2.950S	decl. wave
166 554	ψ_1	560	0.074	elliptic wave of $^sK_1$
275 555	K_2	525	0.689L 0.320S	decl. wave
056 554	S_a	365	0.316	solar elliptic wave
273 555	S_2	280	3.708	solar principal wave
163 555	P_1	221	3.087	solar principal wave
167 555	Φ_1	221	0.133	declination solar wave
274 554	R_2	215	0.031	minor elliptic wave of S_2
057 555	Ssa	183	1.920	solar declination wave
272 556	T_2	158	0.221	major solar elliptic wave of S_2
265 455	L_2	28.9	0.226	elliptic wave of S_2
065 455	M_m	27.0	2.183	elliptic wave
175 455	J_1	26.7	0.520	elliptic wave of K_1
255 555	M_2	14.0	7.958	principal lunar wave
145 555	O_1	13.8	6.611	principal lunar wave
075 555	M_f	13.6	1.710	declination wave
245 655	N_2	9.2	1.525	major elliptic wave
135 655	Q_1	9.1	1.262	elliptic wave of O_1
235 755	$2N_2$	6.9	0.200	elliptic wave of M_2

TABLE 2.2 Perturbations in Inclination and Node of degree 2.

Semi-diurnal species (m = 2)

$$\dot{I}_{2210} = -\frac{3n}{2}\left[\frac{ae}{a}\right]^2 \frac{\sin I}{(1-e^2)^2}\left[-C_{22}\sin 2(\Omega-\vartheta) + S_{22}\cos 2(\Omega-\vartheta)\right]$$

$$\dot{\Omega}_{2210} = \frac{3n}{2}\left[\frac{ae}{a}\right]^2 \frac{\cos I}{(1-e^2)^2}\left[C_{22}\cos 2(\Omega-\vartheta) + S_{22}\sin 2(\Omega-\vartheta)\right]$$

Diurnal species (m 1)

$$\dot{I}_{2110} = \frac{3n}{2}\left[\frac{ae}{a}\right]^2 \frac{\cos I}{(1-e^2)^2}\left[S_{21}\sin(\Omega-\vartheta) + C_{21}\cos(\Omega-\vartheta)\right]$$

$$\dot{\Omega}_{2110} = \frac{3n}{2}\left[\frac{ae}{a}\right]^2 \frac{\cos 2I}{(1-e^2)^2 \sin I}\left[S_{21}\cos(\Omega-\vartheta) - C_{21}\sin(\Omega-\vartheta)\right]$$

Secular species (m=2)

$$\dot{I}_{2010} = 0$$

$$\dot{\Omega}_{2010} = \frac{3n}{2}\left[\frac{ae}{a}\right]^2 \frac{\cos I\, C_{20}}{(1-e^2)^2}$$

where

$C_{2m} = \mathrm{Re}\,(\mathcal{C}_{2m} + \Delta\mathcal{C}_{2m})$

$S_{2m} = -\,\mathrm{Im}\,(\mathcal{C}_{2m} + \Delta\mathcal{C}_{2m})$

TABLE 2.3 Amplitude and period of solid earth tidal perturbation on LAGEOS inclination and node.

Symbol	T(days)	$\dot{I}$ (10^{-14} rad/s)	$\dot{\Omega}$	δI (10^{-3} arcsec)	$\delta\Omega$
Res_1	1240	0.473	1.128	105	249
K_1	1049	3.483	8.302	651	1552
Res_2	909	0.061	0.144	10	23
ψ_1	560	0.002	0.004	2	4
K_2	525	0.257	0.093	24	9
Sa	365	-	0.002	-	0.1
S_2	280	1.595	0.580	80	29
P_1	221	0.248	0.591	10	23
Φ_1	221	0.003	0.007	0.1	0.3
R_2	215	0.008	0.003	0.3	0.1
Ssa	183	-	0.013	-	0.4
T_2	158	0.056	0.020	2	0.6
L_2	28.9	0.057	0.021	0.3	0.1
Mm	27.0	-	0.015	-	0.1
J_1	26.7	0.012	0.029	0.1	0.3
M_2	14.0	3.422	1.246	9	3
O_1	13.8	0.047	0.113	0.1	0.3
Mf	13.6	-	0.011	-	0
N_2	9.2	0.388	0.141	1	0.3
Q_1	9.1	0.029	0.070	0	0.1
$2N_2$	6.9	0.051	0.019	0.1	0

TABLE 3.1 Adopted Model for the MERIT Solution

Reference System

Equator and Equinox	1950
Lunar and Planetary Ephemeris	NASA-JPL DE 118
Nutation	IAU 1980
Nominal Station Coordinates	NASA-GSFC solution Matera Latitude and Longitude and GORF Latitude fixed.

Dynamical Model

Gm of earth	$3.986004358*10^{14}$ m^3/s^2
earth equatorial radius	6378144.11 m
Gravity model	PGS 1680 (20X20) with selected coefficents to degree 30 and order 28.
Solid earth and Ocean Tide model	MERIT standards augmented of N_2 and K_2 solid earth tides
Love number k_2	0.29 (nominal)
Love and Shida number h_2, l_2	MERIT standards

Measurement Model for Normal Point Generation

Marini-Murray refraction model,with correction for variable laser wavelength

Center of mass correction 0.239 m

66788 normal points, 3 min. bin, from NASA-DIS full rate data.

Data span: September 1983- November 1984.

Algorithm for Normal Point Generation: Recommendations of 5th International Laser Ranging Workshop at RGO (1984).

TABLE 4.1 Polar motion differences with VLBI(NGS)

	X_p(marcsec)		Yp(marcsec)	
Series	*mean*	*rms*	*mean*	*rms*
this solution	-4.3	3.8	5.0	5.6
GSFC	1.0	2.5	25.0	2.0
DGFI	-9.0	2.3	7.0	2.5
CSR	-8.0	2.1	0.0	2.3
UP-TPZ69	0.8	6.5	13.6	5.6

TABLE 4.2 Amplitude and Phase of Annual and Chandler Components of Polar Motion -amplitude and offset in marcsec; phases in degrees-

a) from x_p time series

		Annual		Chandler	
	offset	*ampl.*	*phase*	*ampl.*	*phase*
This solution	42.1	53.47	-0.40	227.1	31.31
(NGS)850ct26	46.5	51.8	1.19	229.2	32.16
(DGFII)85L03	35.3	53.0	2.35	228.7	30.93
(GSFC)85L01	35.4	52.7	2.62	228.4	30.81
(CSR)84L02	35.7	52.4	6.09	229.9	30.03
(IPMS)83A01	36.2	43.8	-.90	235.3	32.85
(BIH)	32.7	74.1	3.06	199.0	30.56
(DGFII)85L02	34.9	54.8	-.17	226.8	31.47

b) from y_p time series

This solution	279.0	42.97	72.62	230.2	126.52
(NGS)850ct26	274.0	40.5	71.57	233.4	127.16
(DGFII)85L03	284.3	45.8	78.52	227.0	126.22
(GSFC)85L01	284.6	47.0	80.75	224.7	125.81
(CSR)84L02	284.7	48.4	81.17	224.0	125.77
(IPMS)83A01	286.0	53.9	88.90	213.7	125.49
(BIH)84A02	284.0	54.4	73.18	212.1	128.84
(DGFII)85L02	284.8	48.1	82.00	224.3	125.54

REFERENCE

(1) Afonso, G., F. Barlier, C. Berger, F. Mignard, J.J. Walch: Reassesment of the Charge and Neutral Drag of LAGEOS and its Geophysical Implications. Journal of Geophysical Research 90, 9381-9398, 1985.

(2) Anselmo, L., P. Farinella, A. Milani, A. M. Nobili: Effects of the Earth Reflected Sunlight on the Orbit of the LAGEOS Spacecraft. Astronomy and Astrophysics 117, 3-8, 1983.

(3) Barlier, F., M. Carpino, P. Farinella, F. Mignard A. Milani, A. M. Nobili: Non-Gravitational perturbations on the semimajor axis of LAGEOS. Annals Geophysical 4A, 193, 210, 1986.

(4) Caporali, A., F. Palutan, A. Cenci, S. Casotto: Pole Position from Laser Ranging to LAGEOS. Proc. of the International Conference on Earth Rotation and the Terrestrial Reference Frame, ed. by I.I. Mueller, 172-189, 1985.

(5) Caporali, A., F. Palutan, A. Cenci, S. Casotto: Polar Motion and European Baselines Determined by Analysis of Satellite Laser Ranging Data. Lettere al Nuovo Cimento 44 , 513-518, 1985.

(6) Cazenave, A., S. Daillet, K. Lambeck: Tidal studies from the perturbations in satellite orbits. Phil. Trans. R. Soc. Lond. A284 595-606, 1977.

(7) Eanes, R. J., Schutz, B.and Tapley, B.: Earth and Ocean Tides Effects on LAGEOS and Starlette. Proc.of the Ninth International Symposium on Earth Tides. E. Schweizerbat'sche Verlags Buchhandlung, Stuttgart 1983.

(8) Goad,C.G.: Application of Digital Filtering to Satellite Geodesy. (Ph. D. Thesis). NOAA Technical Report NOS 71 NGS 6, 1977.

(9) Lambeck, K.: The Earth's Variable Rotation. Geophysical causes and consequences. Cambridge University Press, 1980.

(10) Lerch, F.J., S.M. Klosko and G.B. Patel: A. Refined Gravity Model from LAGEOS (GEM L2) NASA Tech.Memo TM 84986, 1983.

(11) Lerch, F. J. , S. M. Klasko, C.A. Wagner and G. B. Patel: On the Accuracy of Recent Goddard Gravity Models. Journal of Geophysical Research 90, 9312-9334, 1985.

(12) Melbourne, W., R. Anderle, M. Feissel, R. King, D. Mc Carthy, D. Smith, B. Tapley, R. Vincente: Project MERIT Standards. U.S. Naval Observatory circular n. 167, Dec. 27, 1983.

(13) Melchior, P. : The Tides of the Planet Earth. Pergamon Press, 1978.

(14) Palutan, F., A. Cenci, S. Casotto and A. Caporali: Operation and Performance of the Matera Laser Station and Estimation of the Position of the European Stations. Nuovo Cimento 9c, 675-689, 1986.

(15) Putney, B.: General Theory of Dynamic Satellite Geodesy. In National Geodetic Satellite Program, NASA SP 365, 319-334, 1977.

(16) Reigber, Ch., G. Balmino, H. Muller, W. Bosch and B. Moynot: GRIM Gravity Model Improvement Using LAGEOS (GRIM3-L1). Journal of Geophysical Research 90, 9285-9300, 1985.

(17) Reigber , Ch., H. Muller, P. Schwintzer, F. H. Massmann, E.C. Paulis: MERIT LAGEOS Laser Ranging Data Analysis at SFB/DGFI. Proc. of the International Conference on Earth Rotation and the Terrestrial Reference Frame, ed. by I.I. Muller, 88-103, 1985.

(18) Rubincam, D.P.: Atmospheric Drag as Cause of the Secular Decrease of the Semimajor Axis of LAGEOS Orbit. Geophysical Research Letters 7, 468, 470, 1980.

(19) Schutz, B.E. , R.J. Eanes and B.D. Tapley: Station Coordinates, Baselines and Earth Rotation from LAGEOS Laser Ranging 1976-1984. Journal of Geophysical Research 90, 9235-9248.

(20) Schwiderski, E. : Atlas of Ocean Tidal Charts and Maps, part I: The Semi-diurnal Principal Lunar Tide M_2. Marine Geodesy 6, 3-4 (1983).

(21) Smith, D.E. and P.J. Dunn: Long Term Evolu- Geophysical Research 7, 437-440, 1980.

(22) Smith, D.E., D.C. Christodoulidis, R. Kolenckiewickz, P.J. Dunn, S.K., Klosko, M.H. Torrence, S. Fricke, S.Blackwell:Global Geodetic Reference Frame From LAGEOS Ranging (SL5.1AP). Journal of Geophysical Research 90, 9221-9233, 1985.

(23) Smith, D.E. , D.C. Christodoulidis, M.H. Torrence,S.M. Klosko and P.J. Dunn: Polar Motion and Length of Day Determination from Satellite Laser Ranging. Proc. of the International Conference on Earth Rotation and the Terrestrial Reference Frame. ed. by I.I. Muller, 142 171, 1985.

(24) Yoder, C.F., Williams, J.G., Parke, M.E. : Tidal Variations of Earth Rotation. Journal of Geophysical Research 86B2, 881-891, 1981.

(25) Yoder, C.F., J.G. Williams, J.O. Dickey, B.E. Schutz, R.J. Eanes, B.D. Tapley: Secular Variation of the Earth J_2 Harmonic Coefficent from LAGEOS and non tidal Acceleration of the Earth Rotation. Nature 303, 757-762, 1983.

(26) Wahr, J.: The Tidal Motions of a Rotating Elliptical, Elastic and Oceanless Earth. (Ph. d. Dissertion), University of Colorado at Boulder, 1979.

(27) Wilkins, G.A. (ed): Project MERIT, IAU-IUGG Joint Working Group on the Rotation of the Earth. Royal Greenwich Observatory, England, 1980.